# EXPERIMENTAL INVESTIGATION OF CONDENSATION HEAT TRANSFER CHARACTERISTICS AND CORROSION RESISTANCE ON COATED TUBE SURFACES

***Shuai WANG****

Huadian Electric Power Research Institute Co., Ltd., Hangzhou, Zhejiang, 310030, China

* Corresponding author: Shuai WANG; E-mail: shuai-wang@chder.com

*The condensation heat transfer characteristics and corrosion resistance of copper, Ni-P-Cu, polytetrafluoroethylene, Ni-P and Ni coated tube surfaces were investigated. The results indicate that condensation heat transfer coefficient of Ni-P-Cu, PTFE, Ni-P and Ni coated tubes grows by 36.8%，29.3%, 19.6% and 7.5% than that of copper tubes, respectively. The phase structure of Ni, Ni-P, Ni-P-Cu and PTFE coated tube surfaces is mixed crystal structure(nanocrystals-based), mixed crystal structure (amorphous-based), amorphous structure and crystal structure, respectively. Compared with Ni coating and Ni-P coated tube surfaces, the condensation droplets outside Ni-P-Cu and PTFE coated tubes are smaller in size, more densely distributed, and fall off more quickly, which can significantly promote dropwise condensation. Ni-P-Cu coated tube surfaces achieve optimal condensation heat transfer. The corrosion speed of copper, Ni, Ni-P, Ni-P-Cu and PTFE coated tubes are 86.5, 42.6, 18.2, 10.7 and 6.1 $mg \cdot dm^{-2} \cdot d^{-1}$, respectively. PTFE coating tubes have the optimal corrosion resistance. Ni-P-Cu and PTFE coated tube surfaces have the best condensation heat transfer characteristics and corrosion resistance, and can be well used in the recovery of waste heat from low-temperature flue gas. The multiple linear regression of the experimental data was carried out to obtain the experimental correlation formula for Nusselt number of convective condensation composite heat transfer for different coated tubes. The relative error between the predicted value and the experimental value is within ±15%.*

Key words*: coating; condensation; heat transfer; corrosion; flue gas; crystal*

## 1. Introduction

Flue gas waste heat is the main application object of waste heat utilization. According to the difficulty of waste heat utilization, flue gas waste heat is divided into three categories: high temperature flue gas waste heat (higher than 600℃), medium temperature flue gas waste heat (200-600℃) and low temperature flue gas waste heat (less than 200℃). The utilization of waste heat from high and medium temperature flue gas has been widely used in the industrial production process. While, the recovery of waste heat from low-temperature flue gas is faced with major problems such as low-temperature corrosion, ash accumulation and poor heat transfer effect. The exhaust temperature of the traditional power station boiler is generally 120-160℃, and the mass fraction of the steam in the

flue gas is about 5%-15%. Reducing the exhaust temperature of the boiler to recover the obvious heat and latent heat of the steam in the flue gas not only improves the thermal efficiency of the boiler, but also recovers part of the acid gas in the flue gas with the condensate.

In order to solve the two problems of poor heat transfer effect and low temperature corrosion, researchers in various countries are trying to find a heat transfer surface that can maintain the dropwise condensation for a long time and has corrosion resistance. The heat transfer coefficient of dropwise condensation is dozens of times higher than that of the common film condensation. However, there are many factors that affect the heat transfer effect of dropwise condensation, and many researchers have carried out a lot of research work. The wet gas convective condensation heat transfer process were studied, respectively, using the theory of mathematical analysis, model, numerical simulation and experimental method[1-3].The corresponding condensation heat transfer coefficient correlations were obtained by them. Dehbi *et al.*[4] summarized the experimental raw data of six researchers and concluded the experimental correlation formula of heat transfer coefficient of convectional condensation with non-condensing gas. The influence of factors such as droplet radius, contact Angle, gas-liquid interfacial mass transfer resistance and wall subcooling on dropwise condensation heat transfer was studied, respectively[5-7]. Vemuri *et al.*[8], Tanasawa *et al.*[9] and Wu *et al.*[10] studied the distribution of droplets on the condensation wall using mode balance theory, micromagnification and random fractal model, respectively. Droplet shedding radius and droplet distribution are crucial factors affecting the effect of dropwise condensation and heat transfer. Droplet growth mainly depends on the direct condensation of steam on the droplet surface at the initial stage of condensation. However, when the droplet size reaches the combined critical size, the combination between adjacent droplet is the main way for droplet growth [11-12].

At present, there are three kinds of surface materials that can realize bead condensation, including organic accelerators, metal compounds and organic polymers. The heat transfer surface was treated with nickel-based permeable layer technology, electroless Ni-P technology, electroless Ni-P-Cu technology and teflon coating technology respectively, and achieved long-term stable dropwise condensation[13-14]. In order to investigate the corrosion resistance of the dropwise condensation surface, the corrosion experiments on the surface of the electroless plating Ni-P and Ni-P-Cu coating were conducted by Xu *et al.*[15] and Liu *et al.*[16]. The results showed that both kinds of coating have obvious corrosion resistance.

Due to the complexity and instability of the process for dropwise condensation heat transfer, there has been almost no successful application in industrialization. The comparative analysis of condensation heat transfer characteristics and corrosion resistance for different surfaces is still very few, and it has appreciable application foreground. In addition, for the design of condensing heat exchanger containing non-condensable gas, there is no corresponding experimental correlation formula. At present, the design is based on the Colburn-Hougen method, which is cumbersome in calculation and has a large error. Therefore, the surfaces of copper tubes was treated by electroless plating Ni, electroless plating Ni-P, electroless plating Ni-P-Cu and PTFE(polytetrafluoroethylene) coating, respectively. The characteristics of convection-condensation heat transfer and corrosion resistance on the surfaces of different tubes were compared and analyzed by simulating the actual flue gas with wet gas (air mixed with water vapor), and the experimental correlation formula of convection-condensation composite heat transfer Nussel number was obtained, which provided auxiliary guidance for the design of condensing heat exchanger.

## 2. Experimental system and methods

### 2.1. Experimental sample

The substrate of the heat exchange tubes used in the experiment is red copper tube, the outer diameter of the tube is 15.88mm, and the wall thickness is 1mm. Ni coating film, Ni-P coating film and Ni-P-Cu coating film are formed on the surface of red copper tube by electroless plating technology, and the coating film thickness is 20 microns. The mass fraction of phosphorus element in the Ni-P coating film is 13.97%, and the mass fraction of copper element in the Ni-P-Cu coating film is 3.96%. PTFE coating film is formed on the surface of red copper tube using ion beam dynamic mixing injection technology. The coating thickness is 10 microns. A mixture of dilute sulfuric acid and NaCl with a mass fraction of 3% was used in the corrosion experiment to simulate the actual corrosion environment of flue gas.

### 2.2. Experimental system

The experimental process of convection-condensation heat transfer is illustrated in Fig.1. The experimental section is arranged horizontally with a single row of 26 heat exchange tubes. The tube spacing is 30 mm and the effective heat exchange length of the single tube is 280 mm. Rubber hose is used to connect the adjacent tubes to facilitate the replacement of other types of experimental tubes.

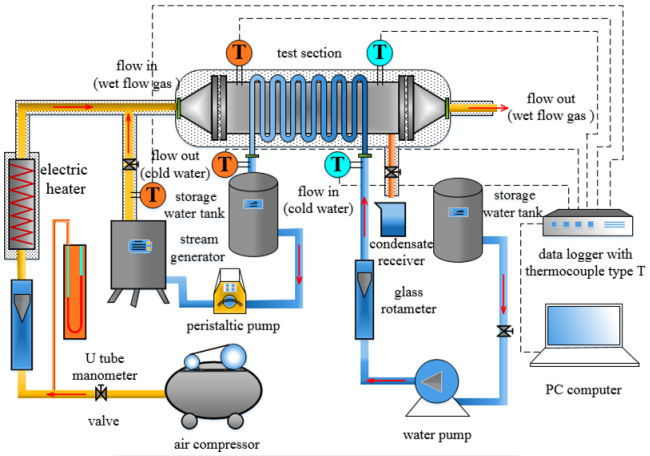


**Fig.1 Schematic diagram of experimental system on convective condensation heat transfer**

The cold air is compressed by the air compressor, and enters the electric heater after the inlet pressure is measured by the u-tube manometer. After heating up, it is mixed with the steam generated by the direct-flow steam generator to form wet gas, whose maximum power is 6kW. The electric heater is adjusted by the XMT-3000B intelligent PID temperature controller to keep the temperature of the wet gas stable at 120℃. The direct-flow steam generator can produce continuous and stable low-pressure steam. A thermocouple is arranged at the steam outlet to monitor the steam temperature. The temperature and humidity transmitter of model HMT337 is used to measure the moisture content of the inlet and outlet of the wet gas in the experimental section, and the relative error is ±1.5%RH. The inlet and outlet temperatures of wet gas and cooling water are measured by copper-constantan thermocouples, and the relative error is ±0.8℃. The condensate water quantity per unit time is measured by means of multiple weighing by electronic balance. In order to minimize the heat loss of the system, the whole experimental system is insulated with thermal insulation cotton.

The acid corrosion resistance of copper tube, PTFE, Ni-P-Cu, Ni-P and Ni coated tube was tested by immersion method. The corrosion rate of different tube surfaces was measured by weighing method, and the changes of surface composition before and after corrosion of them were measured by EDX (Energy Dispersive X-ray Detector). The mechanism of corrosion resistance of different coated tube surfaces was analyzed according to the experimental results.

### 2.3. Measurement methods

The heat absorption of cooling water $Q_c$ is as follows.

$$Q_c = C_{pc} q_{mc} (T_2 - T_1) \quad (1)$$

Where, $C_{pc}$ is the specific heat capacity at constant pressure of cooling water at qualitative temperature, [J·kg$^{-1}$·K$^{-1}$]. Qualitative temperature of cooling water $T=(T_1+T_2)/2$.

The heat exchange on the wet gas $Q_a$ is as follows.

$$Q_a = q_a (h' - h'') \quad (2)$$

Where, $h'$ , $h''$ are the inlet and outlet enthalpy of wet air, [J·kg$^{-1}$]. According to the law of conservation of energy, the heat transfer by convective condensation outside the tube in the experimental section should be equal to the heat absorbed by the cooling water in the tube as follows.

$$Q_a = Q_c \quad (3)$$

The relative error of thermal balance is calculated as follows.

$$\sigma = \left| \frac{Q_a - Q_c}{\frac{Q_a + Q_c}{2}} \right| \le 10\% \quad (4)$$

According to the heat balance theory, Eq. (3) is valid in theory. Due to the system's heat dissipation to the outside and the existence of measurement errors, the calculated heat release and heat absorption are not completely equal. Therefore, the following equation is used to determine the total heat transfer $Q$.

$$Q = \frac{Q_a + Q_c}{2} \quad (5)$$

The latent heat $Q_l$ is as follows.

$$Q_l = m_c h_l \quad (6)$$

Condensation heat transfer coefficient $h_c$ is as follows.

$$h_c = \frac{Q_l}{A_o \Delta t} \quad (7)$$

$$\Delta t = \frac{t_{s1} + t_{wo}}{2} - \overline{t_w} \quad (8)$$

Since wet gas will carry a small amount of condensed water droplets on the pipe wall, resulting in a large error in the measurement of moisture content and dew point temperature at the outlet, the condensation heat transfer temperature difference is calculated according to Eq. (8).

Because the thickness of the coating layer is micron, so the calculation of the outer wall area of the tubes can ignore the thickness of the coating layer, which is easy to simplify the calculation. The

total heat transfer coefficient between the wet gas outside the pipe and the cooling water inside the pipe is as follows.

$$K = \frac{Q}{A_o \Delta t_m} \tag{9}$$

$$\Delta t_m = \frac{(t_1 - T_2) - (t_2 - T_1)}{\ln \frac{t_1 - T_2}{t_2 - T_1}} \tag{10}$$

Where, $\Delta t_m$ is the logarithmic average temperature difference between the inner and outer fluids.

The heat transfer coefficient of convection inside the tube is calculated using Gnielinski formula.

$$Nu_i = \frac{(f/8)(Re_l - 1000)Pr_l}{1 + 12.7\sqrt{f/8}(Pr_l^{2/3} - 1)} \left[ 1 + \left( \frac{d_i}{L} \right)^{2/3} \right] c_t \tag{11}$$

$$h_i = \frac{Nu_i \lambda_l}{d_i} \tag{12}$$

Where, $f$ is Darcy resistance coefficient for fluid flow in the tube; $Re_l$ is Reynolds number of cooling water; $Pr_l$ is the Prandtl number of cooling water under the qualitative temperature; $\lambda_l$ is the thermal conductivity of cooling water at a qualitative temperature, $W \cdot m^{-1} \cdot K^{-1}$。

The convection-condensation composite heat transfer coefficient $h_o$ outside the tube is obtained by extrapolation method as follows.

$$h_o = \frac{1}{\frac{1}{K} - \frac{d_o}{2\lambda_{dc}} \ln \frac{d_o + 2\delta_{dc}}{d_o} - \frac{d_o}{2\lambda_w} \ln \frac{d_o}{d_i} - \frac{1}{h_i} \frac{d_o}{d_i}} \tag{13}$$

The different tube surfaces were immersed in the corrosion medium at the temperature of 25 ℃. After 168 hours, electronic balance was used to weigh the samples before and after immersion. The corrosion rate is as follows.

$$V_{cor} = \frac{m_1 - m_2}{A \cdot S} \tag{14}$$

## 3. Experimental results and discussion

### 3.1. Heat transfer characteristics of coated tube surfaces

#### *3.1.1 Condensation heat transfer characteristics*

Fig.2 presents the condensation heat transfer characteristics of different tube surfaces when the mass fraction of wet gas vapor is 5%, 10% and 15%, respectively. The results indicate that condensation heat transfer coefficient of Ni-P-Cu, PTFE, Ni-P and Ni coated tubes grows by 36.8%，29.3%, 19.6% and 7.5% than that of copper tubes, respectively. Moreover, it can be seen that the higher the mass fraction of water vapor is, the better the condensation heat transfer effect is. The main reason is that the higher the mass fraction of water vapor is, the higher the dewpoint temperature is, and the lower the content of non-condensable gas is. The thinner the thickness of non-condensable gas layer near the wall is, the better the condensation heat transfer effect is. The condensation heat

transfer effect of Ni-P-Cu coated tube surfaces is the best, followed by PTFE coated tube surfaces. With the increase of water vapor mass fraction and Reynolds number, the condensation heat transfer effect of them is more prominent than that of other tube surfaces.

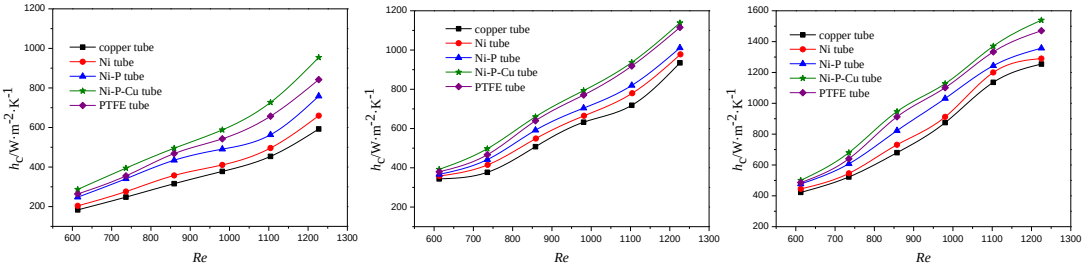


(a) mass fraction of water vapor is 5% (b) mass fraction of water vapor is 10% (c) mass fraction of water vapor is 15%

**Fig.2 Condensation heat transfer coefficient vs Reynolds number of wet flow gas**

When the mass fraction of water vapor is 10% and the Reynolds number is 980, the condensation state outside the tube surfaces of different tube surfaces is presented in Fig.3. It can be obviously obtained that condensation state of Ni, Ni-P, Ni-P-Cu and PTFE coated tube surfaces is mainly dropwise condensation, while the condensation state of copper tube is mainly filmwise condensation. Compared with Ni and Ni-P coated tube surfaces, the condensate droplets outside Ni-P-Cu and PTFE coated tube surfaces have smaller particle size and denser distribution. The smaller droplet diameter and denser droplet distribution indicate that the heat transfer have better condensation heat transfer effect.

The condensation rate (that is, the weight of water vapor condensed into droplets per unit time) can more accurately reflect the condensation heat transfer effect. When the mass fraction of water vapor containing wet gas is 10% and the Reynolds number is 980, the condensate water is collected and weighed by the collector repeatedly. The results show that the average condensation rate of copper, Ni, Ni-P, Ni-P-Cu and PTFE coated tube surfaces are 21.56, 22.35, 23.42, 25.97 and 24.81g/min, respectively. Therefore, drops on Ni-P-Cu and PTFE coated tube surfaces fall off at a smaller diameter and a faster rate, which lead to better condensation heat transfer effect. Ni-P-Cu coated tube surfaces achieve optimal condensation heat transfer.

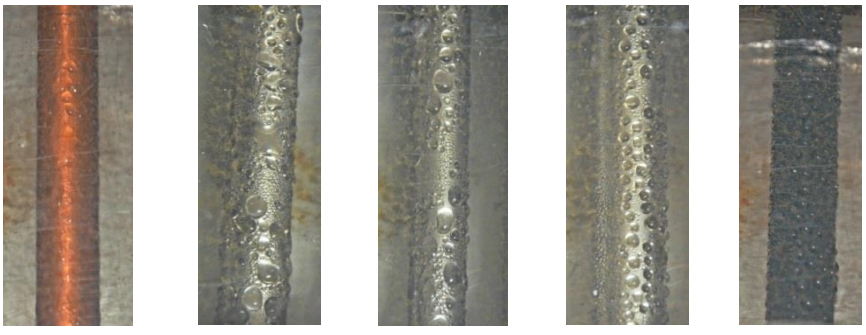

(a) copper tube (b) Ni tube (c) Ni-P tube (d) Ni-P-Cu tube (e) PTFE tube

**Fig.3 Condensation pattern outside different tube surfaces**

The performance of coating to promote dropwise condensation is generally determined by its structure and composition. As shown in Fig.4, the phase structures of different tube surfaces were analyzed by XRD, respectively. The results indicate that the surface of the copper tube presents obvious and sharp diffraction peaks near $2\theta$=43°, 50° and 74°, corresponding to Cu(111), Cu(200) and

Cu(220) crystal planes, respectively. The half-height and width of the strongest diffraction peak is 0.32°, so the surface of the copper tube is a typical crystal structure. There is only a sharp diffraction peak near $2\theta$=45° in the Ni coating film, corresponding to the Ni(111) crystal plane, with half high width of 2.96°. Due to the larger half high width, the surface of Ni coating film is mainly composed of nanocrystalline structure, with a small amount of amorphous structure. Ni-P coating has not been clear crystal diffraction peak, but there is an approximate symmetrical distribution of diffuse scattering "steamed bread peak" near $2\theta$= 45°, with half high width of 4.51°, but the "peak" steamed bread have a relatively sharp diffraction peak, which diffraction peak position corresponds to Ni (111). It belongs to a finer crystal size of nano-sized nickel; hence the structure of the Ni-P coating surface is a mixed crystal structure composed of nanocrystals and amorphous, mainly the amorphous structure. There is no obvious and sharp diffraction peak in the XRD diffraction curve of the Ni-P-Cu coated surfaces, but there is a "steamed bread peak" near $2\theta$=45°, whose half high width is 5.56°, and it has no relatively sharp diffraction peak. Therefore, the atoms on the surface of the Ni-P-Cu coating film are arranged in a disordered state in space, which is an amorphous structure.

The reduction of crystal content in the coating and the increase of amorphous content will reduce the surface free energy of the condensation heat transfer surface. The lower surface free energy will decrease the shedding diameter and increase the shedding frequency of the droplets on the condensation heat transfer surface. The surface of copper tube is crystal structure, the surface free energy is high and the condensation form is mainly film condensation. Ni coating surface is nanocrystalline structure, containing a small amount of amorphous structure and it can promote dropwise condensation. Its condensation heat transfer effect is better than copper tube. The surface of Ni-P coated tube is of mixed crystal structure (mainly amorphous structure). The content of amorphous on the surface of Ni-P coated tube is higher than that on the surface of Ni coated film. Therefore, the free energy on the surface of Ni-P coated tube is correspondingly lower than that on the surface of Ni coated film. The surface of Ni-P-Cu coated tube is amorphous structure, and its crystal content is lower than that of Ni-P coated tube. Therefore, the free energy on the surface of Ni-P-Cu coated tube is correspondingly lower than that on the surface of Ni-P coated tube. The dropwise condensation effect is better than that of Ni-P coated tube.

Moreover, it is also noted from Fig.4 that the relatively obvious diffraction peak of PTFE coating only appears near $2\theta$=18°, corresponding to the PTFE(100) crystal plane. The half high width of the diffraction peak is 0.29°. Therefore, PTFE coating is also crystal structure, the main reason is that PTFE's non-branching symmetric main chain structure makes it highly crystalline. However, the electronegativity of fluorine atoms in PTFE is extremely great, and the perfect symmetry of tetrafluoroethylene monomer makes PTFE surface free energy lower. The lower surface free energy can increase the contact angle of liquid on the solid surface and significantly promote the dropwise condensation.

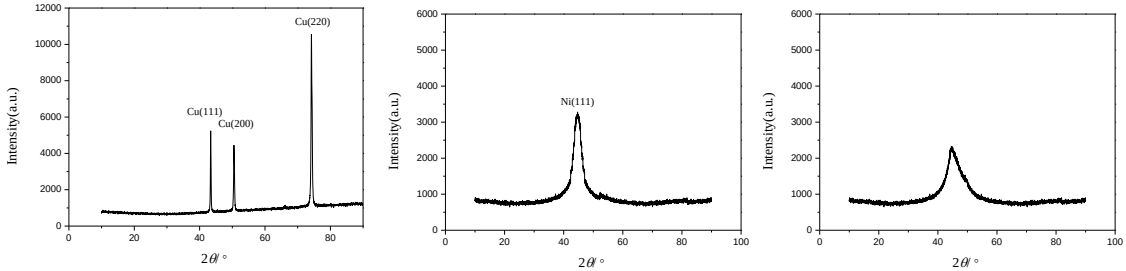


(a) Copper tube (b) Ni tube (c) Ni-P tube

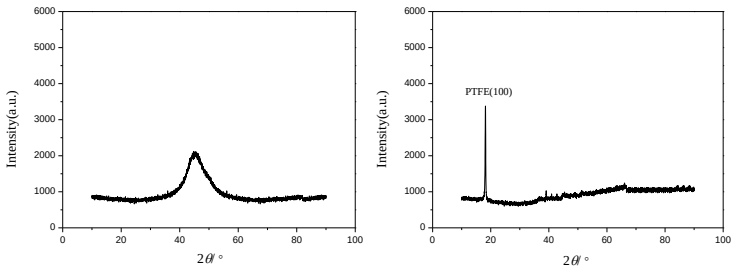


(d) Ni-P-Cu tube (e) PTFE tube

**Fig.4 XRD diffraction curves of different tube surfaces**

### *3.1.2 Convection-condensation heat transfer characteristics*

Fig.5 shows the relationship between the convection-condensation composite heat transfer coefficient of different tube surfaces and the Reynolds number of wet gas when the water vapor mass fraction is 5%, 10% and 15%, respectively. It can be seen that the velocity of wet gas and the mass fraction of water vapor are two important factors affecting the heat transfer coefficient of convection-condensation. The influence of water vapor mass fraction on the heat transfer coefficient of convection-condensation is much greater than that of the velocity of the wet gas. This is mainly because the mass fraction of water vapor in the wet gas is small, and the main factor limiting the increase of heat transfer intensity is the mass fraction of water vapor.

It can also be seen from Fig.5 that the convection-condensation heat transfer coefficient of Ni-P-Cu coated tubes is the largest, followed by PTFE, Ni-P and Ni coated tubes. When the mass fraction of water vapor is 15% and the Reynolds number is greater than 857, the increase rate of the convectional-condensation heat transfer coefficient becomes slower and slower. The main reason is that the main factor affecting the condensation rate is the condensation area when the water vapor mass fraction and Reynolds number are high. The condensation rate of water vapor decreases as the condensation area approaches saturation.

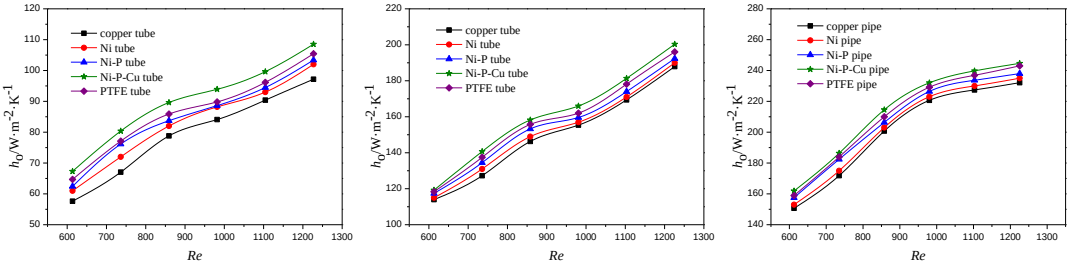


(a) mass fraction of water vapor is 5% (b) mass fraction of water vapor is 10% (c) mass fraction of water vapor is 15%

**Fig.5 Convection condensation heat transfer coefficient vs Reynolds number of wet flow gas**

At present, the Colburn-Hougen method is widely used in the design of condensing heat exchangers containing non-condensable gases, but the calculation process is complicated and the error is large. Based on the theoretical derivation of the Colburn-Hougen model, Da[17] obtained a dimensionless criterion (*Ln*) to measure the heat transfer effect of convection-condensation.

$$Ln = \frac{T_{\mathrm{sat}(\mathrm{P_v})} - T_{\mathrm{w}}}{T_{\mathrm{g}} - T_{\mathrm{w}}} \tag{15}$$

Where, $T_{\mathrm{sat(Pv)}}$ is the saturation temperature corresponding to the partial pressure of water vapor; $T_{\mathrm{w}}$ is the wall temperature; $T_{\mathrm{g}}$ is the main flow temperature of mixed gas.

According to the experimental data of convection-condensation heat transfer of different tube surfaces, multiple linear regression is carried out for the dimensionless criterion Eq.(15). Experimental correlation formulas of convection-condensation heat transfer Nussle number for copper, Ni, Ni-P, Ni-P-Cu and PTFE coated tubes are showed as follows.

$$Nu = CRe^{n}Pr^{m}Ln^{P} \tag{16}$$

$$Nu_{\mathrm{Cu}} = 1.180Re^{1.621}Pr^{1/3}Ln^{1.183} \tag{17}$$

$$Nu_{\mathrm{Ni}} = 0.310Re^{1.064}Pr^{1/3}Ln^{1.061} \tag{18}$$

$$Nu_{\mathrm{Ni\text{-}P}} = 0.394Re^{1.031}Pr^{1/3}Ln^{1.056} \tag{19}$$

$$Nu_{\mathrm{Ni\text{-}P\text{-}Cu}} = 0.413Re^{1.016}Pr^{1/3}Ln^{0.976} \tag{20}$$

$$Nu_{\mathrm{PTFE}} = 0.378Re^{1.039}Pr^{1/3}Ln^{1.032} \tag{21}$$

The applicable conditions of the experimental correlation formulas are that the Reynolds number is 600-1300 and the water vapor mass fraction is 5%-15%. As shown in Fig.6, the relative error between the predicted value and the experimental value was within ±15%.

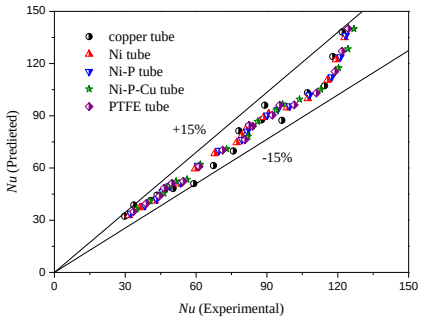


**Fig.6 The predicted results vs experimental results of convection condensation heat transfer**

### *3.1.3 Total heat transfer characteristics*

Fig.7 schematically shows the total heat transfer characteristics of different coated tubes when the mass fraction of wet gas vapor is 5%, 10% and 15%, respectively. It can be found that the total heat transfer coefficient of PTFE coated tubes is higher than Ni-P and Ni coated tubes, and lower than Ni-P-Cu tubes. The results also indicate that the total heat transfer coefficient curves of copper, Ni-P-Cu, PTFE, Ni-P and Ni coated tubes are basically consistent with the trend of the convection-condensation composite heat transfer coefficient curves. The main reason is that the convective heat transfer coefficient in the tube is basically the same, and the heat transfer resistance of the gas side is the largest in the whole heat transfer process.

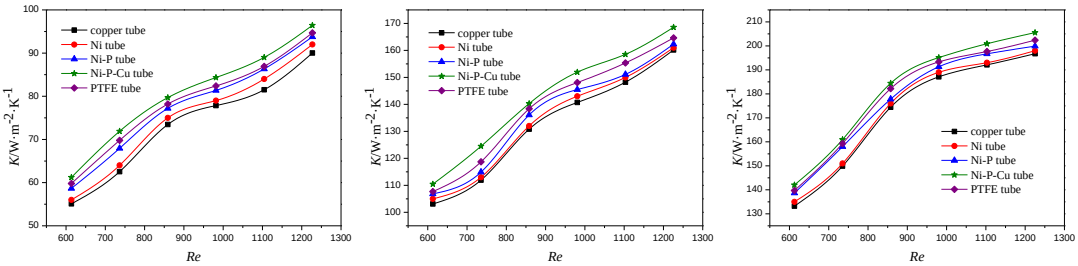


(a) mass fraction of water vapor is 5% (b) mass fraction of water vapor is 10% (c) mass fraction of water vapor is 15%

**Fig.7 Total heat transfer coefficient vs Reynolds number of wet flow gas**

Through the study of convection-condensation heat transfer characteristics of different coated tubes, it can be seen that Ni-P-Cu and PTFE coated tubes have obvious performance of promoting dropwise condensation and good convection-condensation heat transfer effect, while Ni-P-Cu coated tubes have the best convection-condensation heat transfer effect.

### 3.2. Corrosion resistance of different coated tube surfaces

The acid corrosion resistance of different coated tube was tested by immersion method. The corrosion rates on the surfaces of different coated tubes were measured by weighing method, as shown in Fig.8. The corrosion speed of copper tubes, Ni, Ni-P, Ni-P-Cu and PTFE coating tubes are 86.5, 42.6, 18.2, 10.7 and 6.1 $mg \cdot dm^{-2} \cdot d^{-1}$, respectively. The comparative analysis shows that PTFE coated tube has the best corrosion resistance, followed by Ni-P-Cu coated tube. Ni-P coated tube and Ni coated tube have relatively weak corrosion resistance.

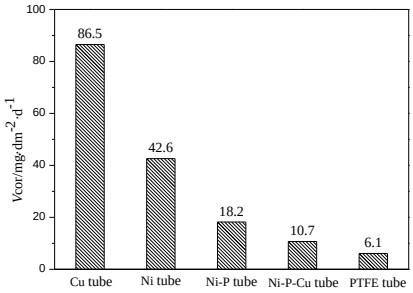


**Fig.8 Corrosion rate of different coated tube surface**

Fig.9 reveals the changes of surface morphology and composition before and after corrosion of different coated tubes. The surface of the copper tube is relatively smooth before corrosion, and the surface presents the state of small particles disorderly stacking after corrosion. Some small voids existed on the surface of Ni coated tube before corrosion, and serious corrosion cracks appeared on the surface after corrosion. The surface of Ni-P coated tube was closely arranged with cellular structure before corrosion, and a slight corrosion crack appeared on the surface after corrosion, and it began to spread to the four sides along with the cellular material. The cellular structure of the micro surface of Ni-P-Cu coated tubes before corrosion was denser than that of Ni-P coated tubes, and the surface after corrosion was very smooth without obvious corrosion crack. There was no significant change in the microstructure of PTFE coated tubes before and after corrosion.

The changes of surface composition before and after corrosion of them were measured by EDX. As can be seen from the figure, the weight percentage of copper element on the surface of copper tube decreased by 35.61% after corrosion, and the weight percentage of chlorine element was 34.86%. The weight percentage of nickel element on the surface of Ni coated tube decreased by 21.54% after corrosion, and the weight percentage of copper element was 21.81%. After corrosion, the weight percentage of nickel on the surface of Ni-P coated tube decreased by 13.80%, and that of phosphorus increased by 7.92%. The surface composition of Ni-P-Cu and PTFE coated tube changed slightly after corrosion.

In combination with the changes in the surface morphology and composition of the coated tube before and after corrosion, it can be seen that the chloride ion in the corrosive medium has a strong penetration capacity. First, the oxide film on the surface of copper tube is damaged and pitting occurs. The resulting corrosion product particles cover the defective surface and form a blocking battery on

the surface of copper tube, further accelerating the corrosion rate. The corrosion medium enters the coating film through the gap on the surface of the Ni coating film, which damages the coating structure and causes the coating film to fail. The chloride ion and the nickel element in the Ni coating form soluble nickel chloride, and the adsorption layer of the subphosphite generated becomes denser by the phosphorus reaction and the film is rich in phosphorus. The subphosphite adsorption layer makes the corrosion resistance of the Ni-P coated tube superior to that of Ni coated tube. The potential of copper element in Ni-P-Cu coating is higher than that of nickel. Many corrosion micro cells are formed on the coating surface with nickel as anode and Cu as cathode. The corrosion products form a $Ni(OH)_2$ film on the coating surface, which retardes the corrosion process and has better corrosion resistance than Ni-P coating. The molecule of PTFE is a spiral conformation formed by the covalent bond of two elements of carbon and fluorine. The fluorine atom almost covers the whole carbon chain skeleton, so that the main chain of the polymer is not invaded by any outside reagent.

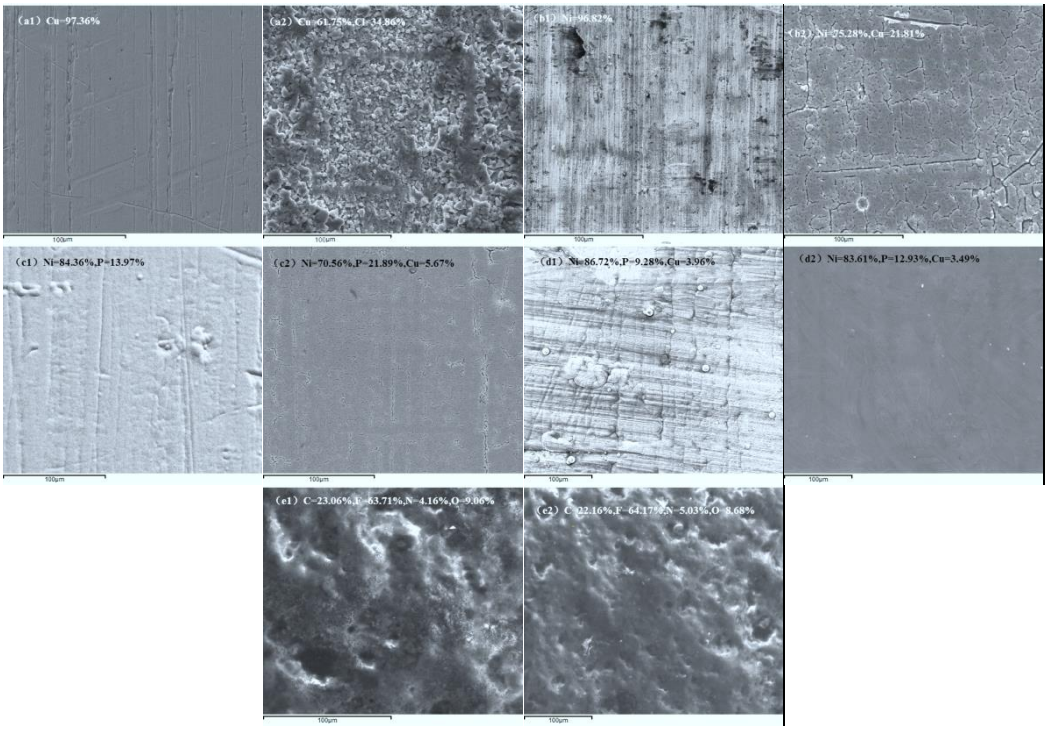


(a) Cu tube, (b) Ni tube, (c) Ni-P tube, (d) Ni-P-Cu tube, (e) PTFE tube;

1- before corrosion; 2- after corrosion

**Fig.9 Morphology and composition of coated tube surfaces before and after corrosion**

## 4. Conclusions

(1) Condensation heat transfer coefficient of Ni-P-Cu, PTFE, Ni-P and Ni coated tubes grows by 36.8%，29.3%, 19.6% and 7.5% than that of copper tubes, respectively. Condensation state of Ni, Ni-P, Ni-P-Cu and PTFE coated tube surfaces is mainly dropwise condensation, while the condensation state of copper tube is mainly filmwise condensation. Compared with Ni coating and Ni-P coating tube surfaces, the condensation droplets outside Ni-P-Cu coating and PTFE coating tubes are smaller in size, more densely distributed, and fall off more quickly. Ni-P-Cu coating tube surfaces achieve optimal condensation heat transfer.

(2) The phase structures of Ni, Ni-P, Ni-P-Cu and PTFE coated tube surfaces are mixed crystal structure(nanocrystals-based), mixed crystal structure(amorphous-based), amorphous structure and crystal structure, respectively. The free energy on the surface of Ni-P-Cu coated tube is correspondingly lower than that on the surface of Ni-P coated tube. The perfect symmetry of tetrafluoroethylene monomer makes PTFE surface free energy lower. The lower surface free energy can increase the contact angle of liquid on the solid surface and significantly promote the dropwise condensation.

(3) The corrosion speed of copper tubes, Ni, Ni-P, Ni-P-Cu and PTFE coating tubes are 86.5, 42.6, 18.2, 10.7 and 6.1 $mg \cdot dm^{-2} \cdot d^{-1}$, respectively. PTFE coated tube has the best corrosion resistance, followed by Ni-P-Cu coated tube. Ni-P coated tube and Ni coated tube have relatively weak corrosion resistance.

(4) Ni-P-Cu and PTFE coating tube surfaces have the best condensation heat transfer characteristics and corrosion resistance, which can be well used in the recovery of waste heat from low-temperature flue gas.

**Nomenclature**

$A$ – corrosion area, [$m^2$]
$A_o$ – area of tube outer wall, [$m^2$]
$d$ – diameters of the heat exchange tube, [m]
$h$ – heat transfer coefficient, [$W \cdot m^{-2} \cdot K^{-1}$]
$h_l$ – specific enthalpy of condensed water, [$kJ \cdot kg^{-1}$]
$m$ – quality, [kg]
$Pr$ – Prandtl number($=\mu C_p/\lambda$), [–]
$Q$ – total heat transfer, [W]
$q$ – mass flow rate, [$kg \cdot s^{-1}$]
$Re$ – Reynolds number ($=UD/n$), [–]
S – corrosion time, [d]
$t$ – temperature of wet gas, [℃]
$T$ – temperature of cooling water, [℃]

***Subscripts***

a – wet gas
c – cooling water
dc – coating
$i$ – inner
o – outer
s1 – dew-point
w – wall surface
1 – inlet
2 – outlet

***Greek symbols***

$\sigma$ –relative error, [%]
$\lambda$ –thermal conductivity, [$W \cdot m^{-1} \cdot K^{-1}$]
$\delta$ –thickness, [m]
$\mu$ –dynamic viscosity, [Pa·s]

**References**


[1] Revankar,S. T., *et al*., Laminar Film Condensation in a Vertical Tube in the Presence of Noncondensable Gas, *Applied Mathematical Modeling*, 29(2005), pp. 341-359

[2] Zheng, S., *et al*., Experimental and Modeling Investigations of Dropwise Condensation Out of Convective Humid Air Flow, *International Journal of Heat and Mass Transfer,* 151(2020), pp.119-129

[3] Li, J., CFD Simulation of Water Vapor Condensation in the Presence of Non-condensable Gas in Vertical Cylindrical Condensers, *International Journal of Heat and Mass Transfer*, 257(2013), pp. 708-721

[4] Dehbi, A., Guentay, S., A Model for the Performance of a Vertical Tube Condenser in the Presence of Noncondensable Gases, *Nuclear Engineering and Design*, 177(1997), pp. 41-52

[5] Hu, H., Tang, G., Theoretical Investigation of Stable Dropwise Condensation Heat Transfer on a Horizontal Tube, *Applied Thermal Engineering*, 62(2014), pp. 671-679

[6] Zheng, S., *et al*., Dropwise Condensation in the Presence of Non-condensable Gas: Interaction Effects of the Droplet Array Using the Distributed Point Sink Method, *International Journal of Heat and Mass Transfer*, 141(2019), pp. 34-47

[7] Alberto, B., *et al.*, Experimental Analysis of Steam Condensation Over Conventional and Superhydrophilic Vertical Surfaces, *Experimental Thermal and Fluid Science*, 68(2015), pp. 216-227

[8] Vemuri, S., *et al*., Long Term Testing for Dropwise Condensation Using Self-assembled Mono Layer Coatings of Noctadeeyl Mercaptan, *Applied Thermal Engineering*, 26(2006), pp. 421-429

[9] Tanasawa, I., *et al*., Experimental Study on Dropwise Condensation, *Bulletin of Japan Society of Mechanical Engineers*, 16(1972), pp. 1184-1188

[10] Wu, Y., *et al*., Effect of Constriction Resistance on Dropwise Condensation Heat Transfer, *Journal of Chemical Industry and Engineering*, 52(2001), 10, pp. 869-901

[11] Xu W., *et al*., Droplet Size Distributions in Dropwise Condensation Heat Transfer: Consideration of Droplet Overlapping and Multiple Re-nucleation, *International Journal of Heat and Mass Transfer*, 127(2018), pp. 44-54

[12] Burnside, B. M., *et al*., Digital Computer Simulation of Dropwise Condensation From Equilibrium Droplet to Detectable Size, *International Journal of Heat and Mass Transfer*, 42(1999), 16, pp. 3137-3146

[13] Cheng, Y., *et al*., Experimental Study on Condensation Heat Transfer of Deposit Heat Exchange Surface, *Proceedings of the CSEE*, 30(2010), 8, pp. 27-31(in chinese language)

[14] Zhang, B., *et al*., Dropwise Steam Condensation on Various Hydrophobic Surfaces：Polyphenylene Sulfide (PPS), Polytetrafluoroethylene (PTFE), and Self-assembled Micro/nano Silver (SAMS), *International Journal of Heat and Mass Transfer*, 89(2015), pp. 353-358

[15] Xu, X., *et al*., The Corrosion Behavior of Electroless Ni-P Coating in $Cl^-/H_2S$ Environment, *Applied Surface Science*, 258(2012), 22, pp. 8802-8806

[16] Liu, G., *et al*., Corrosion Behavior of Electroless Deposited Ni-Cu-P Coating in Flue Gas Condensate, *Surface and Coatings Technology*, 204(2010), 21, pp. 3382-3386(in chinese language)

[17] Da, Y., *et al*., An Experimental Study on Forced Convection-condensation Heat Transfer of the Flue Gas with High Moisture, *Industrial Boiler*, 1(2003), pp. 12-15(in chinese language)